One-dimensional harmonically confined SU(*N*) fermions

M. C. Gordillo ⬤

Departamento de Sistemas Físicos Químicos y Naturales, Universidad Pablo de Olavide, 41013 Sevilla, Spain

F. Mazzanti and J. Boronat

Departament de Física, Universitat Politècnica de Catalunya, Campus Nord B4-B5, E-08034 Barcelona, Spain

We study the momentum distributions and spatial correlations of few harmonically confined SU(*N*) fermions using quantum Monte Carlo methods. In our study, we vary the spin degeneracy *N* from 2 to 6 and the total number of particles from 6 to 18. Only balanced mixtures, with the same number of atoms per spin type, and repulsive unlike-spin contact interactions are considered. Going from $N = 2$ to $N = 6$, with the same occupancy of each spin state, we observe an increase of atom-atom correlations. This effect is particularly significant in the momentum distributions, which show fatter tails at large k ($k\sigma > 5$, σ being the oscillator length) when N grows, in agreement with experimental findings. Those tails also show the expected k^{-4} decay related to the Tan contact for different values of the spin degeneracy. According to our results, the local spin ordering and the spin-spin correlations are mainly determined by N via the Pauli exclusion principle, with minor influences from the particle-particle interactions, irrespective of the total number of confined atoms.

I. INTRODUCTION

The experimental realization of ultracold confined gases of alkali-earth atoms has opened a wealth of studies on multispin systems [1]. Fermionic isotopes of these atoms have orbital degrees of freedom which are largely decoupled from the nuclear spin *I*. In those, one can have at hand a mixture of particles of different spin with the same scattering parameters. Up to now, these have been achieved for ^{173}Yb [2] (not really an alkali-metal atom, but with the same behavior), with $I = 5/2$, and ^{87}Sr [3], with $I = 9/2$. In the experiments, one can populate any number of states up to the maximum spin degeneracy, $N = 2I + 1$, providing a unique setup to study multispin Fermi systems beyond the standard $N = 2$ case achieved much before using alkali atoms such as ^{6}Li or ^{40}K [4]. These unique properties can help future developments in atomic clocks [3,5] and quantum simulators [1,6].

SU(*N*) Fermi mixtures present enhanced many-body correlations in comparison to SU(2) ones, thus making mean-field theory less accurate to describe them [7,8]. In addition, these correlations can be even more relevant in reduced dimensionality [9]. This effect has been observed recently in a quasi-one-dimensional geometry of confined ^{173}Yb atoms which implements a Fermi SU(*N*) system [2]. By progressively populating larger *N* states, that enhancement of correlations produces momentum distributions with larger occupations at higher momenta.

One-dimensional trapped SU(*N*) fermions have been studied in the past using different approaches. Matveeva and Astrakharchik [9] studied the change in the Tan's contact with *N* in the range 2–6 using the diffusion Monte Carlo (DMC) method. Decamp *et al.* [8] also calculated the Tan's contact and the momentum distribution of particles for different degeneracies up to $N = 6$. A relevant result of Ref. [8] is

the prediction of the scaling of the Tan's contact at strong couplings. Both Refs. [8] and [9] are extensions of previous studies on the relation of the Tan's constant to the energies, the tail of the momentum distributions, and other observables in both three-dimensional [10] and one-dimensional SU(2) systems [10–13].

One-dimensional SU(*N*) Fermi mixtures ($N > 2$) can be studied using the same kind of Hamiltonian previously used in the literature for SU(2) [14–18]. Including harmonic confinement, it reads [8,9]

$$HT = \sum_{i=1}^{N_p} \left[\frac{-\hbar^2}{2m}\nabla_i^2 + \frac{1}{2}m\omega^2 x_i^2 \right]$$
$$+ g_{1D} \sum_{\alpha=1}^{N} \sum_{\beta>\alpha}^{N} \sum_{i=1}^{N_\alpha} \sum_{j=1}^{N_\beta} \delta(x_i^\alpha - x_j^\beta), \qquad (1)$$

where *m* is the mass of all fermions, and $g_{1D} = -2\hbar^2/ma_{1D}$ sets the strength of the interaction between particles of spin α and β, with $\alpha \neq \beta$. $N_p = \sum_{\alpha=1}^{N} N_\alpha$ is the total number of confined atoms, with N_α the number of spins of type α. We take the same mass *m* and *s*-wave scattering length a_{1D} for all the fermions, regardless of its spin, and restrict our study to repulsive fermions ($g_{1D} \geqslant 0$) which correspond to $a_{1D} < 0$. We considered g_{1D} values in the range 0–$50\hbar\omega\sigma$ (see below). The one-dimensional (1D) scattering lengths can be readily varied from their 3D counterparts [19] using a confining-induced resonance [20]. However, in alkaline-earth atoms, the use of magnetic fields to tune the scattering length is not possible due to their close electronic shells [1]. Optical resonances can be used, but at the price of significant atom losses. Here, we considered only balanced mixtures, i.e., $N_p = N\,N_1$, with N_1 being the number of atoms with spin

of type 1. According to the Lieb-Mattis theorem and its extensions, balanced configurations, in which the total spin equals 0, should be the ground states for systems including different types of spins [21,22]. All distances are given in units of the oscillator length σ, ($\sigma^2 = \hbar/m\omega$), and the energies in units of $\hbar\omega$, with ω the oscillator frequency.

In this work, we aim to describe the behavior of 1D harmonically confined SU(N) fermions with N_p between 6 and 18, with N in the range 2 to 6. In this way, we extend previous studies in two directions: larger number of particles and interaction regime beyond the limit $1/g_{1D} \to 0$ [8,23]. It is worth noticing that a SU(N) fermionic system made up of N particles is not different than a cluster of N bosons. Since we considered arrangements with $N_\alpha > 1$, fully fermionic behavior was seen for some observables, such as the momentum distributions. The plan of the paper is as follows: In Sec. II, we describe the application of the quantum Monte Carlo method to this problem. The results obtained are discussed in Sec. III, where we report results for the momentum distributions, the Tan's contact, and the relative ordering of atoms as a function of the unlike-spin interaction parameter. Finally, Sec. IV comprises the main conclusions of our work.

II. METHOD

Our theoretical approach is microscopic and it is intended for an exact solution of the many-body Hamiltonian (1). To this end, we rely on the diffusion Monte Carlo (DMC) method, which stochastically solves the many-body Schrödinger equation. In the case of bosons, the DMC method provides exact results within some statistical noise. The study of fermions faces the famous sign problem, which hinders an exact solution with some exceptions, most remarkably 1D systems such as the ones we are considering in this work. To keep the sign under control and avoid the cancellation of signal with growing imaginary time, one normally fixes the nodal surface, where the function is zero, to be the one of a known model. This is the well-known fixed-node approximation, which is known to provide a rigorous upper bound to the exact energy of the system [24]. Generally, the exact ground-state nodal surface is not known and one approximates it as accurately as possible. Fortunately, the situation in one-dimensional fermions is much easier because we know that the nodal points are exactly the points where two particles meet, i.e., when $(x_i^\alpha - x_j^\alpha) = 0$ [25]. The DMC method uses an importance sampling trial wave function to reduce the variance and to introduce the right quantum symmetry. In the present case, we work with a Jastrow-Slater wave function which implements the Fermi statistics by using a Slater determinant for particles with the same spin. This determinant fulfills the condition of the 1D nodes and so DMC is able to find the exact ground-state energy of the system, always within some unavoidable statistical noise. In our calculations, the trial wave function is chosen to be

$$\Phi(x_1, \ldots, x_N) = \prod_{\alpha=1}^{N} D^\alpha \prod_i^{N_\alpha} \prod_j^{N_\beta} \psi\left(x_i^\alpha - x_j^\beta\right). \quad (2)$$

In Eq. (2), the Slater determinants D^α are built with the lowest-energy orbitals of the harmonic oscillator for each species

α. The Jastrow term $\psi(x_i^\alpha - x_j^\beta)$ is chosen as the two-body solution of the Schrödinger equation, without the harmonic potential [14–18],

$$\psi(x_i - x_j) = \begin{cases} \cos(k[|x_i - x_j| - R_m]), & |x_i - x_j| < R_m \\ 1, & |x_i - x_j| \geqslant R_m, \end{cases} \quad (3)$$

in which R_m is a parameter in the range 6–10 σ that is variationally optimized. The parameter k in Eq. (3) is the solution of the equation

$$k a_{1D} \tan(k R_m) = 1, \quad (4)$$

for each value of g_{1D}.

One of our goals in this work is to study how the relative positions of the atoms depended on N, N_p, and the number of atoms per spin. We are mainly interested in topological ordering, i.e., we consider only the spin sequences and not the actual distances between particles. In order to fully characterize the atom distributions, we use both the density profiles and the momentum distributions, $n_\alpha(k)$, of each spin species. The function $n_\alpha(k)$ is the Fourier transform of the one-body density matrix, $\rho_\alpha(x, x')$,

$$n_\alpha(k) = \frac{1}{2\pi} \int dx dx' \rho_\alpha(x, x') \exp[-ik(x - x')], \quad (5)$$

with

$$\rho_\alpha(x, x') = N_\alpha \int dx_2 \ldots dx_{N_p} \Psi(x, \ldots, x_{N_p}) \Psi(x', \ldots, x_{N_p}), \quad (6)$$

which in a cluster depends on both x and x', and not only on the distance between both positions, as in a homogeneous system. $\Psi(x, \ldots, x_{N_p})$ represents the ground-state wave function of the set of atoms, as sampled in the DMC method.

III. RESULTS

Arguably, the first parameter one can think of to characterize the confined SU(N) system, and the primary output of any DMC calculation, is the total energy. We show the energies as a function of the g_{1D} parameter in Fig. 1 for two different values of the total number of particles ($N_p = 12, 18$) and different number of spin components. For $N = 2$, the results are in line with those of smaller systems [15], i.e., the energy is a monotonous function of the interaction parameter that converges to the Tonks-Girardeau (TG) limit [26] for $g_{1D} \to \infty$. That limit depends only on N_p, irrespective of the number of species and on the fermionic or bosonic nature of the interacting particles. For the cluster sizes analyzed, the TG energies are $72\hbar\omega$ ($N_p = 12$) and $162\hbar\omega$ ($N_p = 18$). In general and as it can be seen from the figure, the energies differ significantly at low g_{1D} for different N, while for $g_{1D} \to \infty$ they all approach the common TG limit. For instance, the energy differences for systems with the same value of g_{1D}, the same number of particles, and different N are below 5% for $g_{1D} > 20\hbar\omega\sigma$. The fact that, all other properties being equal, the energy for an arrangement with SU(N) symmetry is smaller than the one for a SU(N') one when $N > N'$ was verified previously only for clusters up to six particles [22].
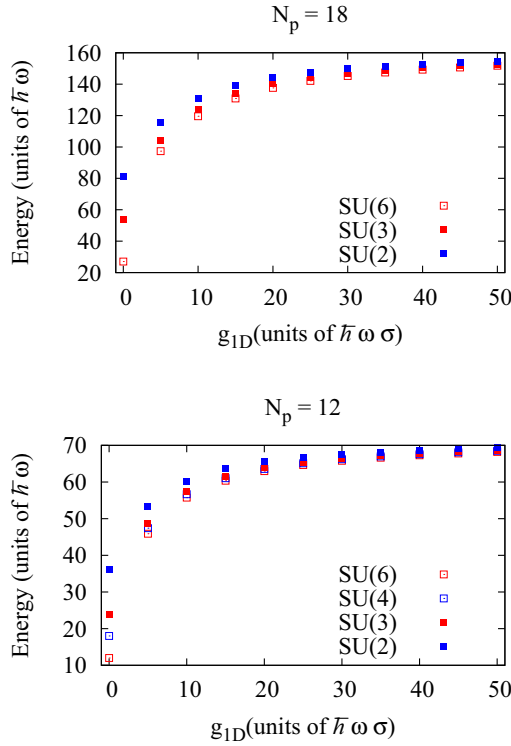
FIG. 1. Total energy as a function of the g_{1D} interaction parameter and for different values of N_p and N in clusters with SU(N) symmetry. Error bars are of the size of the symbols and not displayed for simplicity.

From the results in the figure, we can obtain the Tan's contact C for different values of the number of particles N_p and the interaction parameter g_{1D}, through the relation [9]

$$C = \frac{dE_0}{da_{1D}} = \frac{mg_{1D}^2}{2\hbar^2} \frac{dE_0}{dg_{1D}}, \tag{7}$$

with E_0 the energy of the system. The results are displayed in Fig. 2. There, the symbols correspond to the numerical derivatives obtained by a finite-difference procedure of the results of Fig. 1. Following the scaling law predicted in Ref. [8] for the highly interacting regime, we plot our results in terms of the scaled x variable $\sigma/(|a_{1D}|N_p^{1/2})$ and y variable C/C_∞, with C_∞ the Tan's contact in the TG limit. We can see that our results collapse to the same curve, within the error bars (represented only in one case for clarity). The dashed line is the analytical derivative of a fit to the energies as a function of a_{1D} for the case $N_p = 18$ SU(6). Fits for arrangements with different N or number of particles are virtually identical and not displayed. We can conclude that our data follow the scaling law of Ref. [8] (deduced for the infinite interaction limit) for number of particles larger than the ones considered in that work ($N_p = 18$ instead of a maximum of $N_p = 12$ of Ref. [8]). The fact that the slopes of the energies collapse as a function of the inverse of the size of the cluster was verified also for small SU(2)–SU(4) clusters in previous works [27] for the limits $g_{1D} \to 0$ and $g_{1D} \to \infty$.

The distribution of atoms in systems with different N is studied using the density profiles and the momentum distributions. In Fig. 3, we report those functions for arrangements
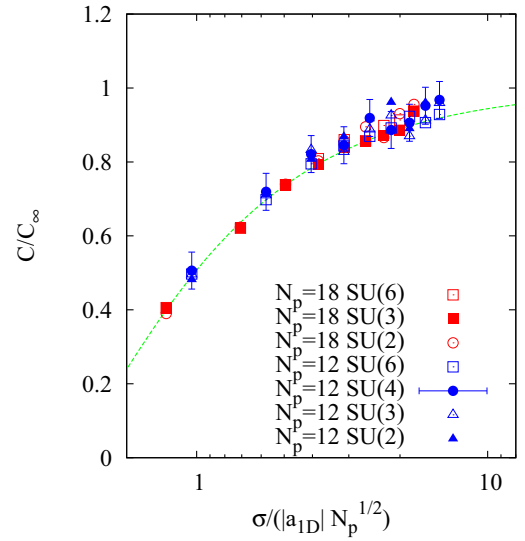

FIG. 2. Ratio between Tan's contact for a given interaction strength, represented by a_{1D}, and the same parameter for $g_{1D} \to \infty$ (C_∞). The dashed line corresponds to the collapsing fits obtained through the derivatives of the data in Fig. 1 with respect to a_{1D}, while the symbols are obtained by deriving numerically the same set of energies.

with the same number of particles per spin (in this case, three) and with N from two to six. The strength of the interaction is taken as $g_{1D} = 10\,\hbar\omega\sigma$, as in Ref. [2], but with a number of atoms per spin channel smaller than 20, the latter being the value reported in the experiment. The density profiles are normalized to the total number of particles, so the widening of the distributions in going from $N_p = 6$ to 18 is to be expected. We also observe that the curves become featureless as to resemble a parabola when the total number of atoms increases. The momentum distributions are normalized to one, as in Ref. [2], and are averages over the N distributions in each cluster. They display a number of maxima in the low-k region equal to the number of atoms per specie (counting both the k and $-k$ values, the latter not shown for the sake of simplicity), in accordance with previous literature. We use a double logarithmic scale to emphasize that for large values of k, the value of $n(k)$ grows with N, in accordance with the experimental findings of Ref. [2]. Therefore, correlations become more important when the spin degeneracy grows. From the data in Fig. 3, we can say that the scaling law that describes the behavior of the long tails of $n(k)$ ($k\sigma > 5$) is also fulfilled in a certain range of large momenta. The dashed straight line in the same figure is $C/(N_p k^4)$, with C the Tan's contact for the SU(4) cluster obtained from data in the previous figure. The N_p factor comes from the normalization to one of the momentum distributions used. The law is fulfilled in other cases, but the dependencies are not displayed for simplicity.

The increase in correlations with N, which makes atoms populate states with larger k in the momentum distributions, can also be seen for the same number of particles, N_p, but different symmetries [SU(6), SU(3) and SU(2)] in the top panel of Fig. 4. In this case, the momentum distributions are normalized to the number of components per spin. For a bulk system, one expects a sharp decrease in occupancy of
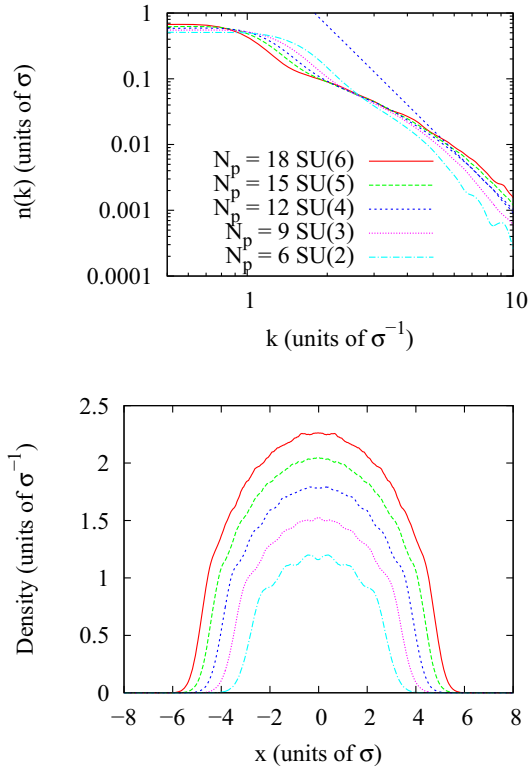
FIG. 3. Top panel: Momentum distributions [$n(k)$] for different N, normalized to one. The straight line corresponds to $C/(12k^4)$ for the SU(4) set of atoms. The interaction parameter is $g_{1D} = 10 \hbar\omega\sigma$. Bottom panel: Density profiles normalized to the number of particles for different N, with $N_p = 18$ and $g_{1D} = 10 \hbar\omega\sigma$.
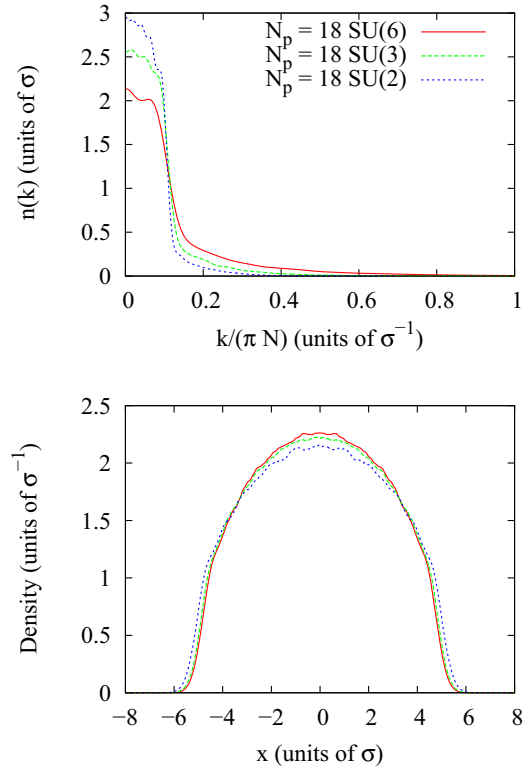

FIG. 4. Same as in the previous figure, but for SU(6), SU(3), and SU(2) clusters with $N_p = 18$ and $g_{1D} = 10\hbar\omega\sigma$. The momentum distributions are normalized to the number of particles per spin component.

the states outside the Fermi sphere of radius, $k_F = \pi\rho/N$, with ρ being the particle density. We therefore scale all momenta with k_F. The result of this procedure is displayed in Fig. 4. There, we can see that there is a clear decrease in the momentum occupation above k_F, as expected, and that the correlations induced by increasing N produce fatter tails for $k > k_F$, as in the case already displayed in Fig. 3.

On the other hand, the density profiles do not change appreciably in going from SU(2) to SU(6), for the same number of particles and the same interparticle interaction, aside from a minor spreading of the function with decreasing N. This can be seen in the bottom panel of Fig. 3.

In 1D Fermi systems, it is also interesting to study the spatial distribution of spins inside different clusters. In contrast to other methods, this is easily calculated in Monte Carlo since, in DMC, one is constantly sampling particle configurations. We study their relative ordering and not the actual distances between consecutive atoms, i.e., we consider topological distances. The first of those distributions is displayed in Fig. 5 for SU(2) with $N_p = 18$ and $N_p = 12$ atoms, and different values of g_{1D}. This figure reports the probability of having another atom of the same spin as an nth neighbor. The first conclusion is readily apparent: the probability of having a nearest neighbor with the same spin is low, and thus the system presents local antiferromagnetic correlations. In fact, that further away probability is basically independent of the topological distance for interacting clusters and only

fluctuates appreciably around a common average for $g_{1D} = 0$. This is something that can be seen experimentally in 1D chains of balanced mixtures of spin-up and spin-down ^{6}Li
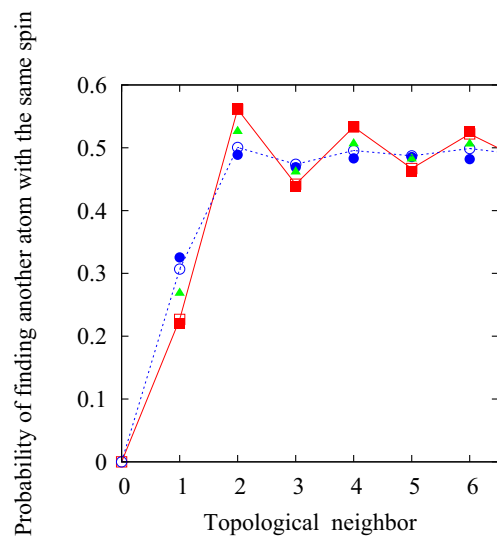

FIG. 5. Probability of finding another spin of the same type as a nth topological neighbor for SU(2) systems. Solid symbols: $N_p = 18$; open symbols: $N_p = 12$. Squares: $g_{1D} = 0$; triangles (only for $N_p = 18$): $g_{1D} = 20\hbar\omega\sigma$; circles: $g_{1D} = 50\hbar\omega\sigma$. The error bars are of the same size as the symbols and not shown for clarity.
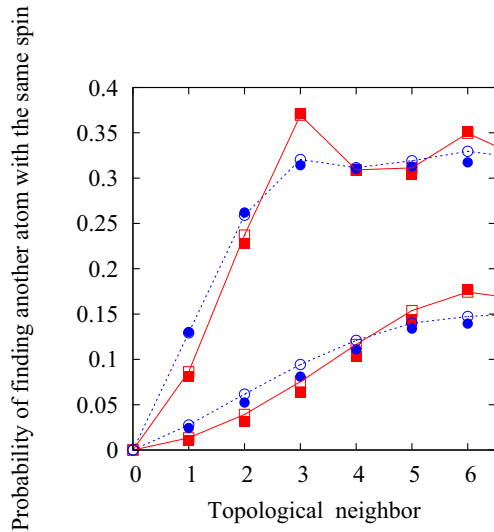
FIG. 6. Same as in the previous figure for SU(3) (upper curves) and SU(6) (lower curves) clusters with $N_p = 18$ (full symbols) and $N_p = 12$ (open ones). Only the cases for $g_{1D} = 0$ and $g_{1D} = 50\hbar\omega\sigma$ are displayed.

FIG. 7. Probability of having a set of N different consecutive neighbors in SU(N) clusters as a function of the g_{1D} parameter. Full symbols: $N_p = 18$; open symbols: $N_p = 12$. Error bars are of the size of the symbols and were not displayed.

atoms loaded in optical lattices interacting repulsively [28]. The first feature can be understood as a direct consequence of the Pauli exclusion principle, which can be thought of as sort of a repulsive interaction for atoms with the same spin. The leveling off of the probability displayed in Fig. 5 from the second position onwards implies that no long-range chain of perfectly alternating ↑↓↑↓↑ ... spins exits. The fact that the distributions are similar for $N_p = 18$ and $N_p = 12$ indicates that this ordering pattern can probably be extrapolated to infinitely long 1D chains, since no obvious size effect appears. We can also see that Pauli's effective repulsion is somehow relaxed when g_{1D} increases, as the local antiferromagnetic correlations are larger in the noninteracting case. The behavior is monotonous with g_{1D}: the values for $g_{1D} = 20\,\hbar\omega\sigma$ are intermediate from those for $g_{1D} = 0$ and $g_{1D} = 50\,\hbar\omega\sigma$.

The SU(3) and SU(6) probabilities for same-spin pairs, as a function of the topological distance, are displayed in Fig. 6. There, only the cases for $g_{1D} = 0$ and $g_{1D} = 50\,\hbar\omega\sigma$ are shown for simplicity since the results for other values of g_{1D} within this range are in between those shown. The general features of the results are similar to their SU(2) counterparts: there is a "hole" in the probability of having another spin of the same type up to the closest $N - 1$ topological position [first and second for SU(3) clusters, and up to fifth in the SU(6) case]. This means that the probability is greatly reduced with respect to what one would expect from a random distribution of spins. As in the previous case, the results are basically independent of the size of the cluster and the avoidance of same-spin neighbors is purely local. The probabilities beyond the Nth neighbor also level off, being their values are above but close to $(N - 1)/(N_p - 1)$, corresponding to a completely random spin distribution.

The existence of a hole for the same-spin probability for close neighbors could lead us to think that the atoms order themselves in "packages" of spins of N atoms of different types. As we can see in Fig. 7, in which we show the
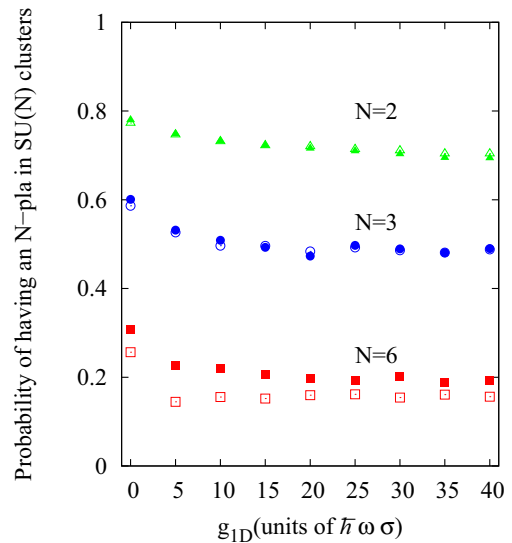
probabilities of having N different consecutive spins in SU(N) clusters as a function of g_{1D}, this is only partially true since that would imply the values of those probabilities are equal to one for any value of g_{1D}, and they are not. As before, we can see that to a very good approximation, they are functions of N and not of the total number of particles, N_p. In fact, the values for $N_p = 12$ and $N_p = 18$ are basically on top of each other for SU(2) and SU(3) clusters. Those probabilities are also practically independent of g_{1D} for $g_{1D} \geqslant 20\hbar\omega\sigma$. This is in line with the long-range ordering probabilities in smaller SU(2) clusters found in Ref. [15]: there, the probability of finding a configuration of regularly alternating spins reaches a plateau for some g_{1D} value, that probability being smaller than the one corresponding to $g_{1D} = 0$.

IV. DISCUSSION

The DMC method allows us to exactly evaluate the most relevant ground-state properties of one-dimensional harmonically confined SU(N) fermions in 1D, and in this work this has been done for a number of species of up to $N = 6$. In this sense, we have extended previous studies of clusters with smaller number of particles or smaller number of spin types, analyzing the energies, the density profiles, and the momentum distributions. In doing so, we have verified that certain scaling relations, as those pertaining to the Tan's contacts (deduced only for the infinite interaction limit) and to the tails of the $n(k)$ distributions, hold for larger spin arrangements than those previously considered in the literature. We have also found that the shape of the density profiles for big enough clusters depends basically on the total number of particles, with minor corrections due to the number of spin types, provided that the unlike-spin interactions are large enough. The minor spreading with decreasing N for clusters with the same number of particles was found experimentally in SU(6) [29]

and SU(4) [30] Mott insulators loaded in three-dimensional optical lattices.

The extension to larger clusters is especially important for the case of $N = 6$, for which the information for $N_p > 6$ is sparse (only energies are reported in Ref. [9]), and null in other quantities as the momentum distributions, in which only the cases for $N = 6$ and $N_p = 6$ have been previously considered [8]. In this work, we report the momentum distributions $n(k)$ of fully fermionic SU(6) arrangements and compare them with clusters with the same number of particles per spin (larger than one) and different number of spin types, corroborating the experimental results of Ref. [2]. In contrast to what one would expect from a mean-field treatment, the enhancement of correlations produced fatter momentum distribution tails with increasing N. However, in our calculations, this effect is relatively small, indicating that the finite temperature in Ref. [2] could be of much relevance. Unfortunately, thermal corrections could not be included in our calculations since our Fixed-node diffusion Monte Carlo (FN-DMC) method converges to the ground state, what means that our description is valid only at $T = 0$.

The DMC algorithm also gives access to the ordering of particles with different spins inside the clusters. This can be done for any values of the interaction between unlike spins, g_{1D}, and of N, in contrast to what has been previously reported in the literature, in which that information is basically restricted to SU(2) systems in the $1/g_{1D} \to 0$ limit [31–33], even though the techniques used can, in principle, be extended to larger values of N. We cannot resort to the Lieb-Mattis theorem or to its extensions to deduce those spin orderings in SU(N) clusters since they state only that configurations with the same number of atoms per spin have lower energies that those corresponding to other arrangements with the same total number of particles [21,22]. In addition, the DMC technique allows us to study correlations between spins, an experimental observable [28], for 1D SU(N) cold fermionic clusters. Our results indicate that for clusters with unlike-spin repulsive interactions, the main driver of the spin ordering is the Pauli exclusion principle. This forbids two atoms with the same spin to be at the same position, therefore creating an effective repulsive interaction that produces a probability hole for same-spin first topological neighbor pairings. For $g_{1D} = 0$, in between those same-spin atoms we can have any number of atoms of different spin type with no energy penalty. That is the reason why the hole goes up to the Nth -1 position from the initial atom. It also explains why the probability of having N different consecutive spins is larger in noninteracting systems.

When $g_{1D} > 0$, the unlike-spin repulsion partially counteracts the effective Pauli correlation (that only forbids two atoms to be at the *same* position), making it indirectly less favorable to have an all-different N-spin pack. However, that repulsion is not enough to modify the size of the probability hole for same-spin first neighbors. As indicated above, the existence of this hole has been experimentally proved [28] in SU(2) systems.

The antiferromagnetic correlation is purely local and unable to produce long-distance ordered spin distributions in the 1D chains analyzed; by that, we mean a sequence of spins of the type $\uparrow\downarrow\uparrow\downarrow\ldots$ spanning the *entire* SU(2) cluster or the equivalent $\uparrow\downarrow\to\uparrow\downarrow\to\ldots$ in a SU(3) one. In that spin basis, those can be defined as pure "antiferromagnetic," in a similar way as is done for an Ising chain. If we had those kinds of distributions, the probabilities displayed in Figs. 5 and 6 would have a distinct sawtooth profile beyond the $N - 1$th neighbor that we do not see. This is in agreement with previous results for small SU(2) clusters (up to four particles) for the $1/g_{1D} \to 0$ limit in which they can be described by a Heisenberg Hamiltonian [31]. The equivalence of the energies obtained in a continuous description and the one afforded by the Heisenberg Hamiltonian has been checked in Refs. [34] and [35] in small (up to four particles) systems by solving the full continuous model. When $g_{1D} > 0$, the coupling constant between fermionic particles is positive, leading to an antiferromagnetic (AFM) Heisenberg chain [22,31,32]. Exact-diagonalization procedures show that the ground states of those Heisenberg clusters are mixtures of all the possible configurations in the spin base, i.e., the $\uparrow\downarrow\uparrow\downarrow$ ordering for a four-particle cluster is by no means the only possibility, in line with our results for larger clusters. This implies a lack of long-distance Ising-like antiferromagnetic ordering. The same results were obtained for continuous Hamiltonians close to the TG limit [33], and for larger SU(2) clusters with different values of g_{1D} [15]. To our knowledge, no studies of the spin ordering (or spin correlation) in the SU(N) Heisenberg chains are available to be compared to our results.

[1] M. A. Cazalilla and A. M. Rey, Rep. Prog. Phys. **77**, 124401 (2014).

[2] G. Pagano, M. Mancini, G. Cappellini, P. Lombardi, F. Schäfer, H. Hu, X. J. Liu, J. Catani, C. Sias, M. Inguscio, and L. Fallani, Nat. Phys. **10**, 198 (2014).

[3] A. Goban, R. B. Hutson, G. E. Marti, S. L. Campbell, M. A. Perlin, P. S. Julienne, J. P. D'Incao, A. M. Rey, and J. Ye, Nature (London) **563**, 369 (2018).

[4] S. Giorgini, L. P. Pitaevskii, and S. Stringari, Rev. Mod. Phys. **80**, 1215 (2008).

[5] A. D. Ludlow, M. M. Boyd, J. Ye, E. Peik, and P. O. Schmidt, Rev. Mod. Phys. **87**, 637 (2015).

[6] A. J. Daley, Quantum Inf. Proc. **10**, 865 (2011).

[7] M. A. Cazalilla, A. F. Ho, and M. Ueda, New J. Phys. **11**, 103033 (2009).

[8] J. Decamp, J. Jünemann, M. Albert, M. Rizzi, A. Minguzzi, and P. Vignolo, Phys. Rev. A **94**, 053614 (2016).

[9] N. Matveeva and G. E. Astrakharchik, New J. Phys. **18**, 065009 (2016).

[10] S. Tan, Ann. Phys. **323**, 2952 (2008).

[11] M. Barth and W. Zwerger, Ann. Phys. **326**, 2544 (2011).

[12] F. Werner and Y. Castin, Phys. Rev. A **86**, 013626 (2012).

[13] M. Valiente, N. T. Zinner, and K. Molmer, Phys. Rev. A **86**, 043616 (2012).

[14] G. E. Astrakharchik, Quantum Monte Carlo study of ultracold gases, Ph.D. thesis, Università degli Studi di Trento, 2004.

[15] C. Carbonell-Coronado, F. De Soto, and M. C. Gordillo, New J. Phys. **18**, 025015 (2016).

[16] M. C. Gordillo and F. De Soto, Phys. Rev. A **96**, 013614 (2017).

[17] M. C. Gordillo, Phys. Rev. A **96**, 033630 (2017).

[18] M. C. Gordillo, J. Phys. B **51**, 155301 (2018).

[19] M. Kitagawa, K. Enomoto, K. Kasa, Y. Takahashi, R. Ciurylo, P. Naidon, and P. S. Julienne, Phys. Rev. A **77**, 012719 (2008).

[20] M. Olshanii, Phys. Rev. Lett. **81**, 938 (1998).

[21] E. H. Lieb and D. Mattis, Phys. Rev. **125**, 164 (1962).

[22] L. Pan, Y. Liu, H. Hu, Y. Zhang, and S. Chen, Phys. Rev. B **96**, 075149 (2017).

[23] J. Decamp, J. Jünemann, M. Albert, M. Rizzi, A. Minguzzi, and P. Vignolo, New J. Phys. **19**, 125001 (2017).

[24] B. L. Hammond, W. A. Lester, Jr., and P. J. Reynolds, *Monte Carlo Methods in Ab Initio Quantum Chemistry* (World Scientific, Singapore, 1994).

[25] D. M. Ceperley, J. Stat. Phys. **63**, 1237 (1991).

[26] M. D. Girardeau, Phys. Rev. A **82**, 011607(R) (2010).

[27] E. K. Laird, Z. Y. Shi, M. M. Parish, and J. Levinsen, Phys. Rev. A **96**, 032701 (2017).

[28] M. Boll, T. A. Hilker, G. Salomon, A. Omran, J. Nespolo, L. Pollet, I. Bloch, and C. Gross, Science **353**, 1257 (2016).

[29] S. Taie, R. Yamazaki, S. Sugawa, and Y. Takahashi, Nat. Phys. **8**, 825 (2012).

[30] H. Ozawa, S. Taie, Y. Takasu, and Y. Takahashi, Phys. Rev. Lett. **121**, 225303 (2018).

[31] F. Deuretzbacher, D. Becker, J. Bjerlin, S. M. Reimann, and L. Santos, Phys. Rev. A **90**, 013611 (2014).

[32] S. Murmann, F. Deuretzbacher, G. Zürn, J. Bjerlin, S. M. Reimann, L. Santos, T. Lompe, and S. Jochim, Phys. Rev. Lett. **115**, 215301 (2015).

[33] A. G. Volosniev, D. V. Fedorov, A. S. Jensen, M. Valiente, and N. T. Zinner, Nat. Commun. **5**, 5300 (2014).

[34] C. Yannouleas, B. B. Brandt, and U. Landman, New J. Phys. **18**, 073018 (2016).

[35] F. Deuretzbacher, D. Becker, J. Bjerlin, S.M. Reimann, and L. Santos, Phys. Rev. A **95**, 043630 (2017).